doi/10.1002/ecs2.4201 by UNIVERSITY OF WISCONSIN-MADISON, Wiley Online Library on [18/01/2023]. See the Terms and Conditions (https://onlinelibrary.wiley.

DOI: 10.1002/ecs2.4201

ARTICLE

Freshwater Ecology



Sediment phosphorus composition controls hot spots and hot moments of internal loading in a temperate reservoir

Ellen A. Albright^{1,2} | Grace M. Wilkinson^{1,2}

Correspondence

Ellen A. Albright Email: ealbright2@wisc.edu

Funding information

Iowa Water Center Graduate Student Supplemental Reserach Competition; National Science Foundation Division of Environmental Biology, Grant/Award Numbers: 1942256, 2200391; National Science Foundation Graduate Research Fellowship Program, Grant/Award Numbers: DGE-1744592, DGE-1747503; University of Wisconsin-Madison; Wisconsin Alumni Research Foundation

Handling Editor: Arial Shogren

Abstract

Phosphorus (P) flux across the sediment-water interface in lakes and reservoirs responds to external perturbations within the context of sediment characteristics. Lentic ecosystems experience profound spatiotemporal heterogeneity in the mechanisms that control sediment P fluxes, likely producing hot spots and hot moments of internal loading. However, spatiotemporal variation in P fluxes remains poorly quantified, particularly in the context of sediment chemistry as a controlling variable. We measured P flux rates and mobile sediment P forms along the longitudinal gradient of a temperate reservoir every 2 months from February to October 2020. Both aerobic and anaerobic processes mobilized sediment P throughout the year. High flux rates at littoral sampling sites (8.4 and 9.7 mg P m⁻² day⁻¹) occurred in late summer under oxic conditions in the overlying water and mobilized labile organic P. High fluxes at the profundal site coincided with hypolimnetic anoxia under ice cover and in mid-summer (11.2 and 17.2 mg P m⁻² day⁻¹, respectively) and released redox-sensitive P. Several high fluxes substantially skewed the flux rate distribution, providing evidence of hot spots and hot moments of internal loading. We further scaled the measured sediment P flux rates to representative areas of the lakebed to estimate internal P loads at an ecosystem scale. We found that P release from littoral sites under oxic conditions in the overlying water had an outsized impact on total loads. Our findings demonstrate the importance of considering spatial and seasonal variation in sediment P pools and fluxes in order to more accurately estimate internal loads and identify the dominant biogeochemical mechanisms involved.

KEYWORDS

dissolved oxygen, phosphorus, reservoir, seasonality, sediments, spatial variation

INTRODUCTION

An ecosystem's response to external perturbations results from the interaction between fast- and slow-acting state variables, which fall along a gradient of turnover times from short to long, respectively (Carpenter & Turner, 2000). Slow variables determine ecosystem context and control how fast variables respond to external drivers (Walker et al., 2012). Understanding how slow and fast variables interact is necessary for the study and management of complex

This is an open access article under the terms of the Creative Commons Attribution License, which permits use, distribution and reproduction in any medium, provided the original work is properly cited.

 $@ \ 2022 \ The \ Authors. \ \textit{Ecosphere} \ published \ by \ Wiley \ Periodicals \ LLC \ on \ behalf \ of \ The \ Ecological \ Society \ of \ America.$

¹Department of Ecology, Evolution and Organismal Biology, Iowa State University, Ames, Iowa, USA

²Center for Limnology, University of Wisconsin-Madison, Madison, Wisconsin, USA

systems (Crépin, 2007; Ward et al., 2019). For example, eutrophication in lakes and reservoirs is often influenced by interacting slow and fast variables at the sediment-water interface. Sediments hold a pool of phosphorus (P), which is the legacy of past external loading and subsequent sedimentation (Søndergaard et al., 2003; Walsh et al., 2018). This P may be retained in sediments or mobilized and released into the overlying water (i.e., internal P loading; Orihel et al., 2017). Within sediments, there are many different P-containing minerals, organic compounds, and surface complexes, which are vulnerable to different mechanisms of internal loading (North et al., 2015; Orihel et al., 2017). As such, the chemical composition of the sediment P pool is a pivotal slow variable that shapes how the rate of P flux from sediments (i.e., the fast variable) responds to fluctuations in external drivers (Carpenter, 2003).

The response of sediment P flux rates to changing dissolved oxygen availability, the result of external drivers, is shaped by forms of P present in the sediment. For example, if redox-sensitive P forms (i.e., those associated with iron or manganese oxides) dominate the sediment P pool, then hypolimnetic oxygen depletion will trigger P release due to reductive dissolution of host minerals (Jensen & Andersen, 1992; Mortimer, 1941). When water-column mixing delivers dissolved oxygen to the sediment surface, oxidized iron and manganese minerals can stabilize P, which may result in sediment P retention. The idea that oxic conditions prevent P release and that internal loading primarily occurs under anoxia is a persistent paradigm in limnology. However, there is ample evidence that internal P loading occurs under a range of dissolved oxygen conditions based on sediment characteristics (Hupfer & Lewandowski, 2008). If sediments hold a large pool of labile organic P, then oxic conditions are expected to mobilize and release P via microbial decomposition and mineralization (Horppila et al., 2017; Joshi et al., 2015). A mixing event that delivers dissolved oxygen to sediments may also result in sediment resuspension, which releases pore water P and increases diffusive P flux through the sediment profile into the overlying water (Tammeorg et al., 2016). In this example, an influx of dissolved oxygen to the lakebed would stimulate rather than suppress internal loading, especially if sediments were disturbed. The relationship between dissolved oxygen and P flux is expected to vary with the composition of the sediment P pool, which is heterogenous across the lakebed and over time (Kowalczewska-Madura et al., 2019; Nowlin et al., 2005). However, it is unclear how the interaction between this slow variable and external drivers influences spatiotemporal variability in sediment P fluxes and what the consequences of this variation are at the ecosystem scale.

Lentic ecosystems are highly variable in space and time. Temperate reservoirs are particularly variable due

to longitudinal gradients in basin morphometry, as well as strong spatial and seasonal variation in thermal mixing, hypolimnetic dissolved oxygen, and organic matter sedimentation (Cardoso-Silva et al., 2018; Hayes et al., 2017; Nowlin et al., 2005). Increasing water depth from riverine to lacustrine regions of a reservoir yields spatial variation in water-column mixing and thus chemical conditions at the sediment-water interface (Hudson & Vandergucht, 2015; Kimmel & Groeger, 1984). Specifically, shallow riverine and transitional sections remain mixed throughout the open water season, usually maintaining oxygenated conditions above sediments. Conversely, the deeper lacustrine region will likely experience at least intermittent thermal stratification, which may result in hypolimnetic dissolved oxygen depletion (Hayes et al., 2017). In short, basin morphometry produces spatial variation in the dynamics of external drivers that influence internal P loading. Organic matter sedimentation also varies along the longitudinal gradient and may impact the composition of the sediment P pool. Riverine segments receive more allochthonous organic matter inputs, while autochthonous material dominates sedimentation in the lacustrine region (Cardoso-Silva et al., 2018; Hayes et al., 2017). Autochthonous organic matter inputs also vary over space and time due to seasonal algal dynamics and spatial heterogeneity in bloom formation (Buelo et al., 2018; Ortiz & Wilkinson, 2021). When combined, spatial and seasonal variation in both redox conditions and the composition of the sediment P pool likely produce hot spots and hot moments of sediment P release.

Hot spots and hot moments are high rates of biogeochemical activity that occur when two reactants are brought together in space and time within an ecosystem (McClain et al., 2003). This biogeochemical phenomenon can be understood within the conceptual framework of fast and slow variables. Specifically, a hot spot-hot moment is the product of an external perturbation delivering a reactant that interacts with the slow variable resulting in a high rate in the fast variable at that moment and location. For example, sudden water-column mixing due to a storm delivers dissolved oxygen to the sediment surface, which is rich in labile organic P, resulting in a spike of sediment P release due to aerobic decomposition and mineralization, as well as increased diffusive P flux due to sediment disturbance (Tammeorg et al., 2016). This external perturbation interacts with the slow variable (i.e., the sediment P pool) and brings two reactants together (i.e., dissolved oxygen and labile organic P), resulting in the hot spot-hot moment of P flux across the sediment-water interface. Hot spots and hot moments disproportionately influence elemental cycles at the ecosystem scale. For example, temperate waterbodies likely experience hot spots and hot moments of sediment P release such that the majority of the total internal P load may be associated with a few key areas of ECOSPHERE 3 of 16

the lakebed and times throughout the year. As such, efforts to control internal P loading would have the greatest impact by focusing on hot spots and hot moments of P release. However, doing so requires an understanding of the underlying mechanisms. Although hot spots and hot moments have been well documented, most studies have focused on carbon and nitrogen cycles in streams and riparian soils, and there has been little consideration of both hot spots and hot moments of P cycling, especially in lentic ecosystems (Bernhardt et al., 2017). Additionally, analyses of the mechanisms that produce hot spots and hot moments in biogeochemical cycles remain scarce, undermining our understanding of these extreme events and how they impact ecosystem function. While the environmental conditions that may produce high rates of sediment P flux in lakes and reservoirs have been well documented, no study to date has explicitly delineated hot spots and hot moments of sediment P release and, more importantly, identified the causal mechanisms of these extreme events.

In order to quantify hot spots and hot moments of sediment P flux and explore the underlying mechanisms, we measured mobile sediment P pools and fluxes over the course of a year and across the lakebed of a temperate reservoir (Figure 1). Specifically, we measured sediment P composition and flux rates at three sites along the longitudinal gradient of the reservoir approximately every other month over the course of 2020, capturing conditions under the ice, as well as thermal mixing and stratification events during the open water season. We asked the following questions: (Q1) When and where do hot spots and hot moments of sediment P flux rates occur, and what are the underlying mechanisms? (Q2) How does the slow variable (i.e., the composition of the sediment P pool) change over space and time, and how do these changes relate to P flux rates? (Q3) How do hot spots and hot moments of internal loading scale to the ecosystem level? We hypothesize that there are hot spots and hot moments in the rates of P flux from sediments that arise from interactions between P speciation and biogeochemical conditions at the sediment-water interface. Over the course of the year, we anticipate that P will be mobilized and released from a variety of sediment P sources. We anticipate that temperature and dissolved oxygen concentrations will be key mechanisms driving internal loading but that the specific effects of these variables will depend on the composition of the sediment P pool. Predicting the occurrence of hot spots and hot moments of internal loading and identifying the causal mechanisms are essential for effectively managing whole-lake P cycling. Our findings demonstrate that the mechanisms driving hot spots and hot moments of internal P loading cannot be understood without capturing

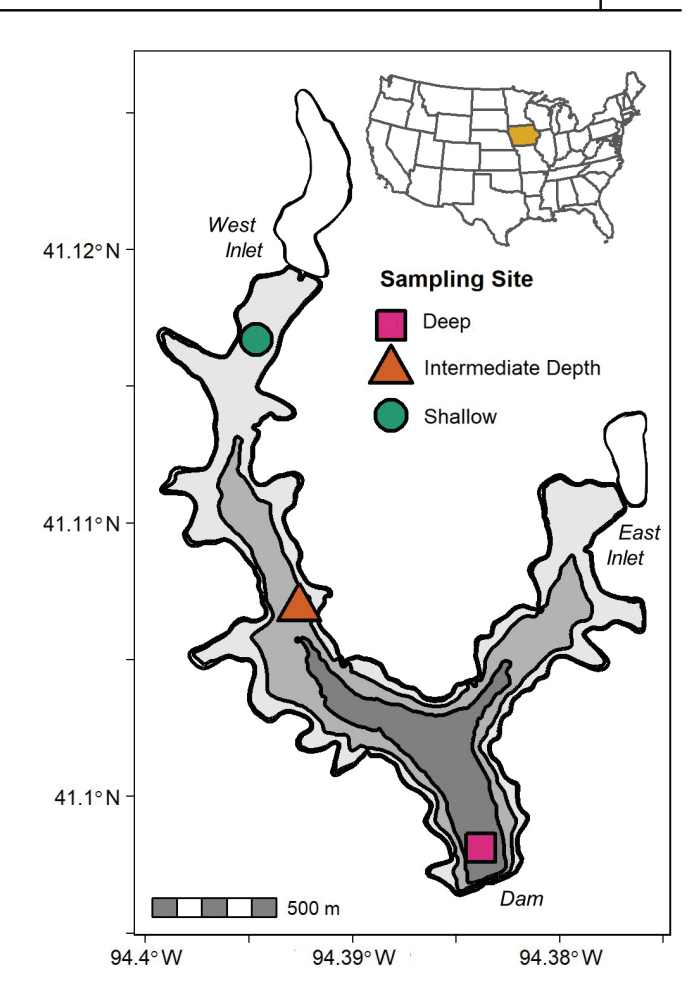


FIGURE 1 Sampling sites in Green Valley Lake, Iowa, USA. The three sampling sites are representative of different areas of the lakebed based on water depth. The shaded polygons illustrate these areas. The shallow site is representative of the 1.2–3.6 m depth contour. The intermediate-depth site is representative of the interval of 3.6–5.6 m, and the deep site is representative of the area deeper than 5.6 m.

both seasonal and spatial variations in fluxes and the composition of the sediment P pool.

METHODS

Study site

Green Valley Lake (GVL) is a hypereutrophic reservoir located in southwest Iowa, USA (41°05′58.9″ N 94°23′04.7″ W; Figure 1), with a discontinuous cold polymictic stratification and mixing pattern. The reservoir lies in the rolling loess prairie region of the western corn belt plains. Row crop agriculture dominates the GVL watershed with 68.4% of the land cover in a corn–soybean rotation. GVL is relatively small (surface area 156.2 ha) and shallow (maximum depth 6.8 m and

mean depth 3.2 m), with two main branches meeting at the southern end of the basin above the dam outflow. As an impoundment of several small tributaries, GVL has a highly irregular shape (shoreline development factor 3.44), characterized by numerous shallow bays and an extensive littoral zone.

We measured spatial variation in sediment P pools and fluxes at three sampling sites distributed along the longitudinal gradient of the west branch of the reservoir. We selected the western branch as this inflow is the main tributary to the reservoir and drains the majority of the watershed. The shallow sampling site (2.5 m) was located near the west inlet, and the water column remained mixed throughout the open water season. The intermediate-depth site (4.0 m) was in the middle of the western branch of GVL. Thermal stratification developed under ice and intermittently throughout the open water season. The deep sampling site (maximum water depth 6.8 m) was located at the deepest hole of the reservoir near the dam. Water-column stratification and mixing followed the same pattern as the intermediate site (Table 1).

In order to evaluate seasonal patterns in P dynamics, we sampled these sites throughout 2020 on days of year (DOY) 39, 117, 181, 223, and 298 that correspond to winter, spring, mid-summer, late summer, and autumn, respectively. The timing of the sampling events was designed to capture ice cover, thermal stratification in spring, and mixing events in the summer and autumn (Table 1). The shallow site was not sampled in February due to unsafe ice conditions created by a congregation of

Canada geese (*Branta canadensis*). The sampling event in late summer occurred immediately following a derecho, an intense windstorm affecting a large geographic area (Corfidi et al., 2016; Goff et al., 2021). Although GVL lies at the edge of the derecho's path, windspeeds at the reservoir are estimated to have exceeded 65 km h⁻¹, fully mixing the water column at all sites (Table 1).

Vertical profiles and water chemistry

To monitor thermal mixing patterns in GVL, we deployed vertical strings of temperature sensors at the shallow and deep sites (HOBO 8K Pendant Temperature Data Logger). Sensors were placed every 0.5 m up to 3 m deep and then every 1 m to the lakebed. The sensors logged water temperature every 30 min from spring to late summer. At each sampling site and event, we also measured water-column profiles of temperature and dissolved oxygen using a YSI ProDSS Multiparameter Digital Water Quality Meter. Additionally, we collected water samples 0.25 m below the water surface and 0.5 m above the sediment-water interface for the analysis of total P (TP), soluble reactive P (SRP), total nitrogen, nitrate, and suspended solids (see Appendix S1 for full methods and data). Subsamples were filtered in the laboratory (0.45-um glass microfiber, GF/C, filters) for SRP analysis, and all samples were preserved with concentrated sulfuric acid to pH 2. TP samples underwent persulfate digestion prior to analysis (Standard Methods for the

TABLE 1 Thermal stratification and dissolved oxygen (DO) conditions at the sediment–water interface.

	Season	Site	Water-column thermal structure	Bottom water		
DOY				Temperature (°C)	DO (mg L ⁻¹)	DO saturation (%)
39	Winter	Intermediate	Stratified	3.2	12.6	94.3
		Deep	Stratified	4.2	1.1	8.6
117	Spring	Shallow	Isothermal	14.6	9.4	92.5
		Intermediate	Stratified	14.1	8.9	86.4
		Deep	Stratified	11.9	5.8	54.3
181	Midsummer	Shallow	Isothermal	26.5	5.4	67.4
		Intermediate	Isothermal	26.3	6.3	78.0
		Deep	Isothermal	24.2	0.3	3.3
223	Late summer	Shallow	Isothermal	26.1	7.2	88.7
		Intermediate	Isothermal	25.4	4.8	58.0
		Deep	Isothermal	24.9	4.5	54.2
298	Autumn	Shallow	Isothermal	6.7	10.2	83.3
		Intermediate	Isothermal	8.1	8.7	73.7
		Deep	Isothermal	8.4	8.7	73.8

Abbreviation: DOY, day of year.

ECOSPHERE 5 of 16

Examination of Water and Wastewater, 1998a). We measured SRP and TP concentrations with the molybdenum blue method modified from Murphy and Riley (1962) and Standard Methods for the Examination of Water and Wastewater (1998b) using a SEAL Analytical AQ2 Discrete Analyzer.

Sediment P fluxes

To quantify sediment P fluxes, we collected intact sediment cores and incubated them under ambient conditions in the laboratory while measuring P exchange with the overlying water. For each sampling site and event, three replicate sediment cores were collected using a gravity corer (inner diameter 5 cm and length 50 cm), such that there were approximately 25 cm of the sediment and 25 cm of the overlying water. The sediment cores and the overlying water were sealed in clear, acrylic core sleeves and transported at 4°C. In the laboratory, we exposed cores to temperature and dissolved oxygen treatments corresponding to ambient conditions at each site (Appendix S1: Table S1, Figure S1). Temperature treatments were achieved by securing the cores in either a water bath or an incubation chamber. Dissolved oxygen levels were manipulated by bubbling either air mixtures or N₂ through the overlying water. A slow, consistent bubble rate was used to gently mix the water column without disturbing the sediment surface. After the cores were placed in the incubation system, we measured the height of the water column within each core tube to calculate the water volume.

Samples of the overlying water were collected 12, 36, 60, and 84 h after the initial incubation setup. For each daily sampling, 50 ml of water was removed for the analysis of TP. An equivalent volume of hypolimnetic water, collected from 0.5 m above the sediment surface at the corresponding site, was used to replace the volume removed. The replacement hypolimnetic water was also analyzed for TP daily to account for changes in water-column P due to sampling and water replacement. Samples were preserved with concentrated sulfuric acid to pH 2 and stored at 4°C before undergoing the persulfate digestion and the analysis for TP (Standard Methods for the Examination of Water and Wastewater, 1998a). We monitored water temperature, dissolved oxygen, and pH (YSI ProDSS Multiparameter Digital Water Quality Meter) daily to ensure that the overlying water remained representative of ambient conditions in the reservoir at the time of sampling.

The change in TP in the overlying water was used to calculate daily areal P flux rates for each core. We determined flux rates based on TP in order to capture all forms

of P that may be exchanged between sediments and the overlying water including phosphate, dissolved organic P forms, and particulate P. We first calculated the mass of P in the overlying water immediately following the collection of the daily water sample, as well as the mass of P in the replacement water. We then determined how the addition of the replacement water changed the TP concentration of the overlying water. The daily change in the TP concentration was calculated as the difference between this new TP concentration after the addition of the replacement water and the TP concentration measured in the water column the next day (see Appendix S1: Equations S1–S4). The P flux rate was then calculated as:

P flux rate
$$(\text{mg P m}^{-2} \text{day}^{-1}) = (C_t - C_0) \times V/A/d,$$
 (1)

where C_t is the water-column TP concentration (in milligrams per liter) on a given day, C_0 is the TP concentration (in milligrams per liter) from the previous day after the addition of the replacement water, V is the total volume (in liters) of the water overlying the sediment core, A is the area (in square meters) of the sediment surface, and d is the number of days between measurements (Ogdahl et al., 2014). Over a 4-day incubation, we calculated three daily P flux rates for each sediment core. We took the mean of these temporal replicates to yield one P flux rate per core, per incubation. The mean flux rate and the standard error of the mean for the three replicate sediment cores from each sampling site and event were then used to estimate the P flux rate through time at various sites.

Sediment P content and composition

At each sampling site and event, we collected an additional sediment core for the analysis of sediment P composition, TP content, and physical characteristics (see Appendix S1 for sediment physical characteristics methods: Equations S5-S7). We extruded the first 10 cm of the sediment profile into an acrylic core sleeve, which was sealed immediately to maintain ambient redox conditions. The top 10 cm of the sediment is considered to be actively exchanging with the overlying water as diffusive processes and turbulent disturbance can occur in sediments this deep (Forsberg, 1989). This surface sediment layer also holds P forms that are likely to be transformed or released on relatively short timescales (Orihel et al., 2017). Samples were transported and stored at 4°C until analysis, which began within 18-36 h of the sample collection. Sediments were handled under N2 atmosphere in a glove bag and thoroughly homogenized before

removing three replicate subsamples from each core. The replicates were analyzed for three mobile P species (loosely bound, redox-sensitive, and labile organic P) and a more stable P fraction (aluminum-bound P) via sequential extraction following Lukkari et al. (2007). Dried sediments were used to quantify TP.

To begin the sequential P extractions, subsamples of the fresh sediment equivalent to 0.5 g of dry sediment were weighed into polyethylene centrifuge tubes. This same sediment pellet was used throughout the sequential extraction procedure. All extractions were performed on an orbital shaker table at 25°C. Extractant and rinse solution volumes (50 ml), shaker table speed (200 rpm), and centrifuge time and speed (30 min at 3000 rpm) were consistent across all extractions. In general, each extraction involved shaking the sediment pellet in the extraction solution, centrifuging, and pouring off the supernatant. All extractions included at least one rinse, in which the sediment pellet would shake for 15 min in a rinse solution to minimize tailing. The supernatant of the rinse extractions was combined with the primary extraction supernatant. Following each extraction, the total supernatant was preserved with concentrated sulfuric acid to pH 2 to keep metals soluble and achieve the required pH for color development during SRP and TP analyses. All SRP and TP concentrations were corrected for the extractant volume and the mass of sediment used to determine the P concentration per gram of dry sediment (see Appendix S1: Equations S8-S13).

Loosely sorbed and pore water P were extracted in 0.46 M N₂-purged sodium chloride (NaCl) for 1 h. One rinse in 0.46 M N₂-purged NaCl was used, and the combined extract solution was preserved for TP analysis (Standard Methods for the Examination of Water and Wastewater, 1998a). Redox-sensitive P species were extracted in a 0.11 M bicarbonate-0.1 M sodium dithionate (BD) solution for 1 h. This extraction included two rinses with BD solution and one NaCl rinse. The combined extract supernatant was bubbled with compressed air for at least 90 min to remove dithionite before being preserved for TP analysis. Labile organic P and P associated with aluminum oxides were determined with an 18-h extraction in 0.1 M sodium hydroxide (NaOH). One NaOH rinse was used, followed by one NaCl rinse. The combined extract supernatant was analyzed in two portions. First, a portion was filtered (0.45-µm GF/C filters) and analyzed for SRP (Standard Methods for the Examination of Water and Wastewater, 1998b). This SRP concentration was used to calculate the sediment concentration of aluminum-bound P. The remaining supernatant was digested and analyzed for TP. The labile organic P fraction was determined as the difference between the total NaOH-extractable P and the aluminum-bound P. Total sediment P concentrations were measured following a hot acid digestion on dried, ground,

and homogenized sediments. Three replicate subsamples (0.2~g) of the dried sediment were combusted at 550° C for 2 h and then boiled on a digestion block in 50 ml of 1 M HCl for 2 h at 150° C. Following digestion, samples were diluted to 50 ml with deionized water and adjusted to pH 2 using 0.1 M NaOH before TP analysis.

Statistical analyses

As there is no universal quantitative method for delineating hot spots and hot moments of biogeochemical fluxes in a distribution of flux measurements (Bernhardt et al., 2017), we used a variety of approaches to explore the distribution of P flux rates and determine whether the observed spatiotemporal variation indicated hot spots or hot moments. We first identified statistical outliers in the distribution, defined as flux measurements falling above or below 1.5 times the interquartile range. We further quantified the shape of the P flux distribution by calculating skewness $(m_3;$ Appendix S1: Equation S14), which identifies whether the distribution is symmetric ($m_3 < 0.5$) or whether extreme flux rates, presumably due to hot spots or moments, skew the distribution ($m_3 > 0.5$). We further evaluated the influence of high flux rates on the distribution by iteratively removing the highest flux rates and recalculating skewness. Through this process, we determined how many of the highest flux rates would need to be removed to produce a nearly symmetric distribution (Gakuruh, 2017).

In order to evaluate how the composition of the sediment P pool varied across sites and seasons, we performed a compositional data analysis. Compositional data analysis tests for a difference in proportions among multivariate observations, allowing us to test differences in the relative abundance of P fractions across different sites and events (Filzmoser et al., 2018). The compositional analysis was defined by concentrations of loosely bound (pore water and surface-sorbed), redox-sensitive (Fe- and Mn-bound), aluminum-bound, and labile organic P. The sediment P concentrations were center-logratio-transformed prior to a principal component analysis (PCA) on the covariance matrix, as not to bias the analysis to the most abundant sediment P fractions.

To estimate the total sediment P load (in kilograms per day) in the reservoir for each sampling event, we multiplied the mean P flux rate (in milligrams per square meter per day) at each sampling site by the lakebed area (in meters) within representative depth contours corresponding to each site. The shallow site measurements were assigned to the 1.2–3.6 m depth contour, the intermediate-depth site measurements were assigned the 3.6–5.6 m depth contour, and the deep site measurements were assigned the 5.6–6.8 m depth contour. The threshold of 5.6 m was determined based on the historical mean depth of hypoxia in the water

ECOSPHERE 7 of 16

column. We excluded areas shallower than 1.2 m, including the sediment retention basins north of the reservoir, because these areas are mainly in secluded, wind-protected bays (Figure 1). Our sampling sites, which were centrally located along a branch of the reservoir, cannot reasonably be extrapolated to these shallow areas due to expected differences in wave disturbance and the depositional environment (Kleeberg et al., 2013). To calculate the lakebed area within the representative depth contours, we used the length of each depth contour from a bathymetric map produced by the Iowa Department of Natural Resources. The area between depth contours is a trapezoid-shaped area of the lakebed wrapping around the reservoir basin. We calculated this area as follows:

$$A = \left(\frac{\text{length } 1 + \text{length } 2}{2}\right) \times h,\tag{2}$$

where length 1 and length 2 are the lengths of the bounding depth contours, and h is the assumed average distance between the depth contours across the lakebed, estimated using the Pythagorean theorem:

$$h = \sqrt{\left(\operatorname{depth} 2 - \operatorname{depth} 1\right)^{2} + \left(\sqrt{\operatorname{area} 1} - \sqrt{\operatorname{area} 2}\right)^{2}}, \quad (3)$$

where depth 1 and depth 2 refer to the water depth of the top and bottom depth contours, and area 1 and area 2 represent the planar areas at the top and bottom depth contours. This method assumes that the lakebed follows a linear slope between the bounding depth contours, so it is likely an underestimate of the true area of the sediment surface. After determining the lakebed area corresponding to each sampling site, we multiplied this area by flux rates and then summed across all three load estimates for the total load for that sampling event. To propagate the uncertainty of this estimate, we added the standard error of mean values in quadrature.

All data are available in Albright and Wilkinson (2021), and the analysis code is available from Zenodo: https://doi.org/10.5281/zenodo.6604143. All analyses were completed in R version 3.6.0 (R Core Team, 2019) using sf (Pebesma, 2018), spData (Bivand et al., 2021), fGarch (Wuertz et al., 2020), robCompositions (Filzmoser et al., 2018), and vegan (Oksanen et al., 2019) packages.

RESULTS

Physiochemical conditions

Water-column chemistry and thermal structure varied across sampling sites and over the course of the year (Table 1). At the shallow site, the water column remained mixed throughout the open water season and the sediment-water interface remained oxic (dissolved oxygen range $5.4-10.2 \text{ mg L}^{-1}$). At the intermediate and deep sites, thermal stratification first developed after ice-off. Intermittent stratification continued through late summer, after which the water column was mixed at both sites. The sediment-water interface at the intermediate-depth site remained oxic throughout the study period (dissolved oxygen range $4.8-12.6 \text{ mg L}^{-1}$), but the deep site experienced periodic hypoxia (dissolved oxygen range $0.3-8.7 \text{ mg L}^{-1}$). On the day of the late-summer sampling (DOY 223), a derecho passed over the reservoir, prompting a mixing event, as evidenced by an isothermal water column at all sampling sites. Following the derecho, the relative contribution of inorganic solids to the total suspended solid pool was much greater than any other point throughout the year in both surface and bottom waters, suggesting that the storm resulted in sediment disturbance and a well-mixed water column (Appendix S1: Table S2).

Hypolimnetic P concentrations followed a similar seasonal pattern across sampling sites (Figure 2). At the deep and intermediate sites, hypolimnetic TP concentrations remained stable between under-ice sampling (DOY 39) and early-spring sampling (DOY 117). Hypolimnetic concentrations of both TP and SRP then increased from spring through late summer, peaking at 318.0–370.9 and 116.3–168.5 $\mu g \ L^{-1}$, respectively, before declining in autumn. Although these nutrient concentrations are quite high, the dynamics of P in the water column in 2020 are consistent with concentrations and seasonal patterns previously measured in GVL (Appendix S1: Figure S2).

Sediment P fluxes

Sediment P flux rates varied substantially among sampling sites and across seasons (Figure 2; Appendix S1: Table S3). Flux rates were most variable over time at the deep site; however, these profundal sediments consistently released P to the overlying water from winter to mid-summer (DOY 39, 117, and 181) and then had moderate retention or release rates in the late summer and autumn (DOY 223 and 298). Sediments from the intermediate-depth site retained P under ice cover (DOY 39) but released P in spring and late summer (DOY 117 and 223). The shallow site followed a similar seasonal pattern with sediment P release in spring and late summer (DOY 117 and 223) and negligible fluxes in mid-summer and autumn (DOY 181 and 298). Overall, the highest rates of P release occurred at the shallow and intermediate sites in late summer (DOY 223) and

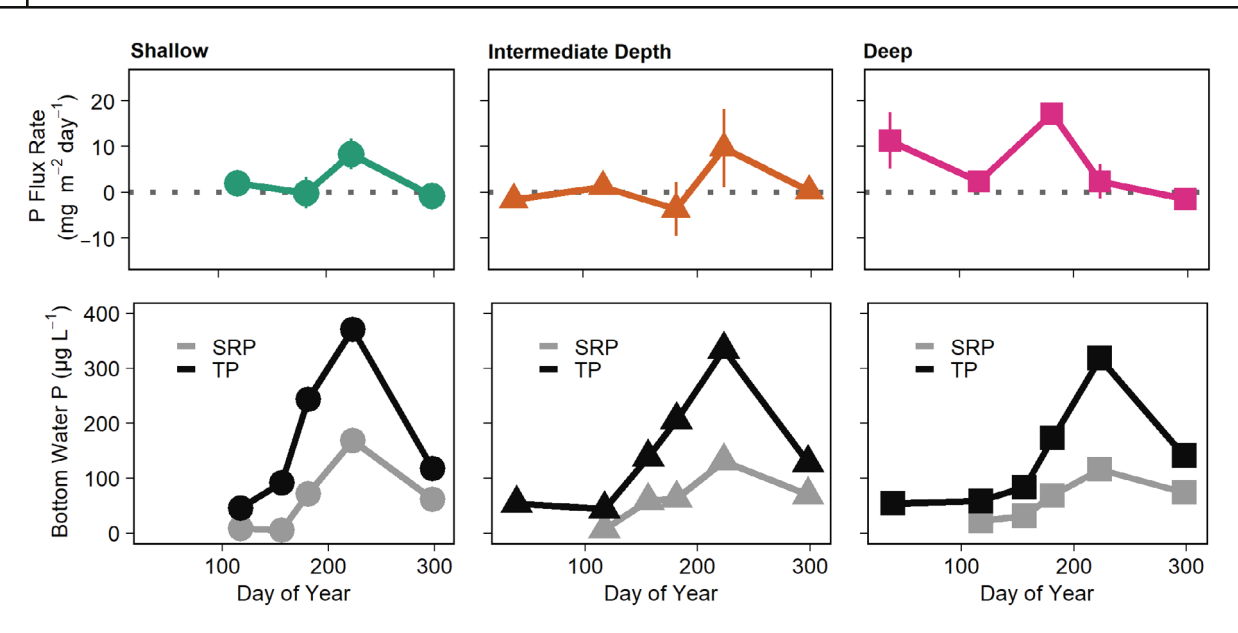


FIGURE 2 Sediment P flux rates and bottom water P concentrations. Top row of panels: Time series of mean sediment total P flux (±SE among three replicate cores) from February to October 2020. The shallow site was not sampled in February due to unsafe ice conditions. Negative values indicate sediment P retention, while positive values show P release. Bottom row of panels: Time series of bottom water total P (TP) and soluble reactive P (SRP) concentrations for each sampling site over the study period.

in winter and mid-summer (DOY 39 and 181) at the deep site.

Over the course of the year, sediment P release occurred under a broad range of dissolved oxygen concentrations at the sediment-water interface (Figure 3, Table 1). At the deep site, nearly anoxic conditions were associated with elevated rates of P release in winter and mid-summer (DOY 39 and 181; dissolved oxygen 1.1 and 0.3 mg L^{-1} , respectively). However, most of the observed instances of P release occurred when oxygen was available at the sediment-water interface. For example, sediments across all three sampling sites released P under oxic conditions in spring (DOY 117; dissolved oxygen range 5.8-9.4 mg L⁻¹), and high rates of oxic P release occurred at the intermediate and shallow sites in late summer (DOY 223; dissolved oxygen 4.8 and 7.2 mg L^{-1} , respectively). The effect of dissolved oxygen availability on sediment P flux rates differed between the deep site and more shallow sampling sites, and elevated P release rates were observed under both oxic and anoxic conditions.

The shape of the distribution of sediment P flux rates over the course of 2020 provides evidence of hot spots and hot moments of sediment P release in GVL. The distribution of P flux rates was centered near 0 mg P m⁻² day⁻¹ with the majority of the rates falling between -10 and 10 mg P m⁻² day⁻¹ (Appendix S1: Figure S3). The first statistical moment, or mean, of the distribution was 3.4 mg P m⁻² day⁻¹. The distribution was moderately positively skewed (third standardized statistical moment $m_3 = 0.818$) due to five high release rates

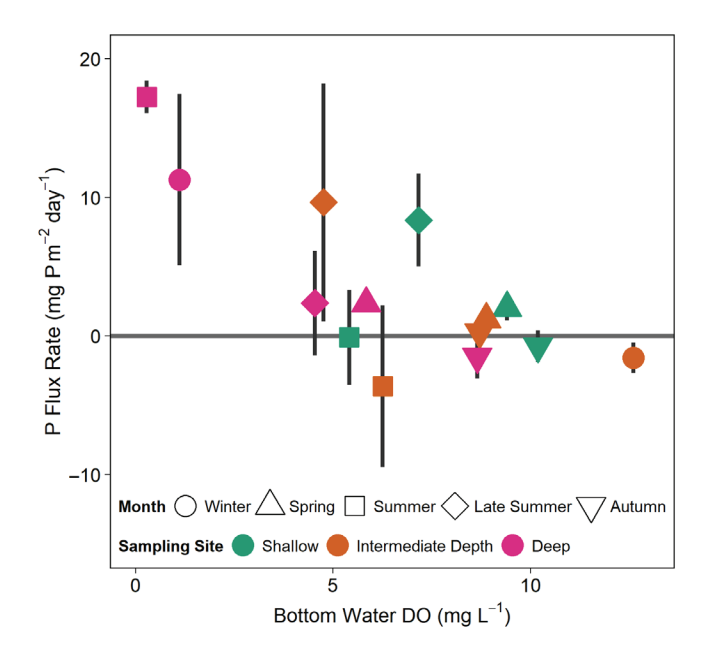


FIGURE 3 Mean sediment P flux rates (±SE among three replicate cores) across the range of observed bottom water dissolved oxygen (DO) concentrations.

(range 16.2–23.6 mg P m⁻² day⁻¹). The four highest of these points were classified as statistical outliers. The high release rates were from the deep sampling site in winter and mid-summer (DOY 39 and 181), as well as fluxes in late summer (DOY 223) from the intermediate and shallow sites (Appendix S1: Figure S4). Subsampling the dataset to exclude the five highest flux rates resulted

ECOSPHERE 9 of 16

in an approximately symmetric distribution ($m_3 = 0.462$; Appendix S1: Table S4). The mean flux rate with five highest rates excluded was 1.2 mg P m⁻² day⁻¹, which is almost a third of the mean flux rate for the whole distribution. The presence of high flux rates that skew the distribution indicates hot spots and hot moments of sediment P release.

Sediment P composition

To understand the spatiotemporal variation in sediment P fluxes, we also measured changes in the sediment P pool, the slow variable, across seasons and sampling sites. The total sediment P pool varied among sites and seasons. Following expected patterns in sediment focusing, TP concentrations increased along the longitudinal gradient of the reservoir and were far greater at the deep site than at the intermediate and shallow sites (Figure 4a). At the deep site, the sediment TP increased slightly from winter to spring (DOY 39-117), decreased between spring and mid-summer (DOY 117-181), and then increased through autumn (DOY 298). At the intermediate side, the TP also increased from winter to spring (DOY 39–117) but then decreased through late summer (DOY 223) before increasing in autumn (DOY 298). The sediment TP decreased gradually from spring to autumn at the shallow site, except for a slight increase between mid- and late summer (DOY 181-223; Appendix S1: Figure S5).

Across all sampling sites, redox-sensitive P was the dominant pool of mobile P found in reservoir sediments constituting an average of 40.9%–51.3% of the TP pool across sites (Figure 4a). The concentrations of all measured sediment P species were dynamic over time across the reservoir. Redox-sensitive P concentrations decreased over the course of the year at the shallow site. At the intermediate-depth site, redox-sensitive P concentrations increased from winter to spring (DOY 39–117), declined through late summer (DOY 223), and increased until autumn (DOY 298). Redox-sensitive P at the deep site declined from winter through late summer (DOY 39–223), before increasing through autumn (DOY 223–298; Figure 4b).

Overall, concentrations of labile organic P increased from spring to autumn at all study sites, except for slight declines between mid-summer and late summer (DOY 181–223) at the intermediate and shallow sites (Figure 4c). Aluminum-bound P concentrations declined from spring through autumn at the shallow site. At the intermediate-depth site, concentrations increased from winter to spring (DOY 39–117), declined through late summer (DOY 223), and then increased again. At the deep site, aluminum-bound P followed an inverse pattern

to that of redox-sensitive P, increasing from winter through late summer (DOY 39–223) and decreasing from late summer to autumn (DOY 223–298; Figure 4d). Temporal patterns in loosely bound P varied across sites with declines over the study period at the shallow site, a gradual increase over time at the intermediate site, and steady concentrations at the deep site except for an increase from late summer to autumn (DOY 223–298; Figure 4e).

We used PCA as part of a compositional data analysis to explore spatiotemporal variation in overall sediment P composition. The compositional analysis was defined by the concentrations of loosely bound, redox-sensitive, aluminum-bound, and labile organic P (Figure 5). The first principal component (PC1) explained 76.77% of the variation in the dataset and was highly correlated with loosely bound and redox-sensitive P contents. The second principal component (PC2) explained 14.35% of the variation and was more closely associated with the labile organic P content. The first two principal components explained 91.12% of the variance in the dataset. Overall, sediment samples from the shallow site had lower loosely bound and redox-sensitive P contents, whereas these species were more prevalent in deep site sediments. The composition of sediments from the intermediate site fell between that of the deep and shallow sites. Over the course of the study period, sediment composition from all study sites generally decreased in loosely bound and redox-sensitive P contents and increased in the labile organic P content.

Sediment physical characteristics remained relatively stable over time but varied along the longitudinal gradient of the reservoir (Appendix S1: Table S5). The loss-on-ignition organic matter content was greatest at the deep site (13.08% \pm 0.98%) and similar between the shallow and intermediate sites (8.83% \pm 0.75% and 8.54% \pm 0.71%, respectively). The water content was also highest at the deep site (86.18% \pm 0.49%) and comparable between the shallow and intermediate sites (71.83% \pm 0.75% and 75.72% \pm 3.0%, respectively). Bulk density decreased from the shallow (1.19 \pm 0.006 g cm $^{-3}$), to the intermediate (1.16 \pm 0.024 g cm $^{-3}$), and to the deep (1.07 \pm 0.003 g cm $^{-3}$) site.

Total P load

We estimated daily sediment P loads for each sampling event by scaling the measured flux rates to representative areas of the lakebed to better understand ecosystem-scale consequences of P fluxes. The estimated TP load across the lakebed varied over time, with higher loads occurring under oxic conditions in spring and late summer (DOY 117 and 223; Figure 6; Appendix S1: Table S6).

10 of 16

FIGURE 4 Spatiotemporal variation in sediment P species. (a) Average, annual sediment P composition by sampling site. Refractory P is estimated as the difference between total P and the sum of the measured P fractions. The relative abundance of each P species as a percent of the total sediment P pool is noted. Time series of mean (±SE of three replicate samples) (b) redox-sensitive, (c) labile organic, (d) aluminum-bound, and (e) loosely bound P concentrations across sampling sites and over the course of the year. Note different y-axis scales across plots depicting more versus less abundant P fractions.

ECOSPHERE 11 of 16

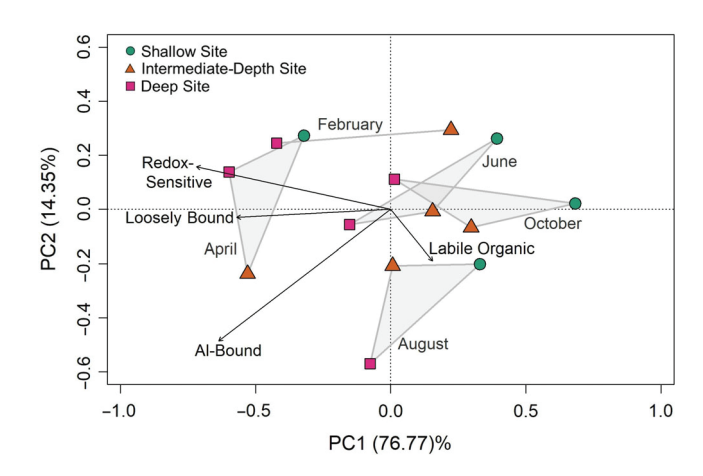


FIGURE 5 Spatiotemporal variation in sediment P composition. Principal components analysis biplot based on a compositional data analysis of sediment P pools over the course of the year and across the reservoir.

The greatest TP load occurred in late summer (DOY 223) due to high flux rates from the shallow and intermediate sites under oxic conditions in the overlying water (Figure 3). Oxic conditions were also associated with high TP loads in spring (DOY 117), when low P release rates across all sampling sites resulted in a substantial TP load due to the large area of the lakebed releasing P. In contrast, high rates of sediment P release under anoxic conditions at the deep site in winter and mid-summer (DOY 39 and 181) did not translate into a high TP load due to the small area of the lakebed involved. The greatest P loads were associated with aerobic sediment P release across a broad area of the lakebed. The seasonal trend in the estimated TP load mirrors the observed time series for hypolimnetic TP and SRP (Figure 2).

DISCUSSION

Hot spots and hot moments of sediment P flux rates

There was clear evidence of hot spots and hot moments of sediment P release in the study reservoir over the course of 2020. These elevated rates of sediment P flux occurred in late summer at the shallow and intermediate-depth sites, as well as in winter and mid-summer at the deep site. While the highest rates of sediment P release occurred under anoxic conditions at the deep site, the other elevated flux rates at the shallow and intermediate sites happened when dissolved oxygen was available at the sediment–water interface. Other studies of hypereutrophic reservoirs have also observed aerobic sediment P release, which was associated

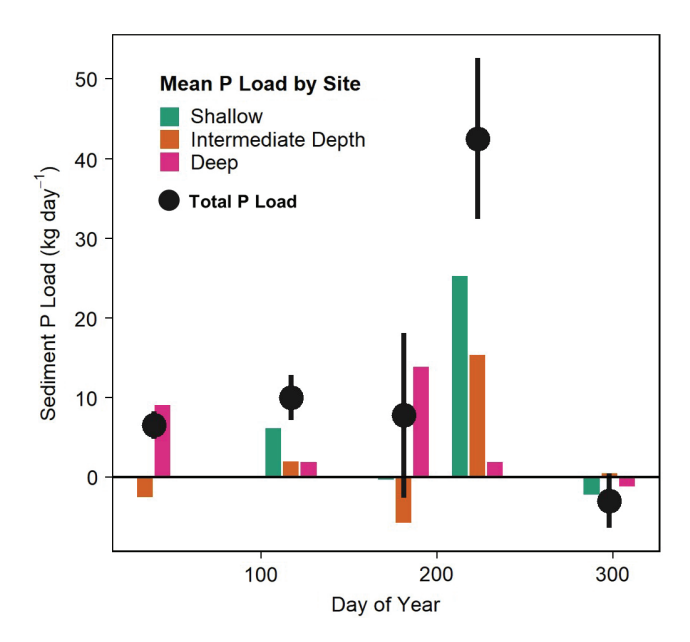


FIGURE 6 Estimated mean P load at the time of sampling by site (bars) and total load across the lakebed (points; error bars are \pm SE). Bar plots show the mean, estimated P load for each sampling site at the time of sampling. Points represent the sum of the estimated loads across the lakebed.

with intense algal production and P mobilization during the decomposition of sediment organic matter (McCarty, 2019; Song & Burgin, 2017). As a hypereutrophic waterbody, GVL also experiences severe algal blooms throughout the summer months, so it is likely that microbial decomposition of algal detritus contributed to the observed aerobic P release.

However, sediment P release when the overlying water is oxic is very complex and may involve both aerobic and anaerobic processes in the sediment profile. The depth of dissolved oxygen penetration into sediments is typically very shallow such that much of the sediment profile remains anoxic (Hupfer & Lewandowski, 2008). Therefore, P mobilization via aerobic decomposition and subsequent mineralization is limited to a thin surficial layer of the sediment. Anaerobic processes of P mobilization, such as the reductive dissolution of redox-sensitive P minerals, can still occur deeper within the sediment profile. The P mobilized via anaerobic processes will diffuse upward and may be released into the overlying water. The P sorption capacity of sediments and the availability of alternative electron acceptors will influence whether mobilized P will diffuse into the overlying water or remain in sediments (Caraco et al., 1993). The observed P release under oxic conditions at the shallow and intermediate-depth sites likely represents P mobilized via aerobic decomposition of sediment organic matter and anaerobic processes within the sediment profile.

A severe storm disturbance on the late-summer sampling date could have further exacerbated internal loading

at the shallow and intermediate sites. The late-summer sampling event occurred immediately following a derecho, which mixed the reservoir water column and disturbed sediments. Sediment resuspension has been shown to increase diffusive P flux from sediments into the overlying water, even after sediments have settled following the disturbance (Tammeorg et al., 2016). Resuspension dilutes the pore water near the sediment surface, prompting diffusion of soluble P from deeper within the sediment profile and thus enhancing diffusive P fluxes into the water column (Tammeorg et al., 2020). It is likely that the high rates of aerobic P release observed at the shallow and intermediate sites in late summer resulted from both P mineralization from organic matter and sediment disturbance brought on by the storm event. Bottom water TP and SRP concentrations also peaked at this time, indicating that these high flux rates influenced whole-reservoir P dynamics.

The highest rates of P flux from the deep site occurred under ice cover and in mid-summer under nearly anoxic conditions at the sediment-water interface. Profundal sediment P release during summer anoxia has been recorded in many other waterbodies and attributed to reductive dissolution of redox-sensitive P minerals (Kowalczewska-Madura et al., 2019; Mortimer, 1941; Nowlin et al., 2005). However, winter measurements of sediment P fluxes are uncommon (Cavaliere & Baulch, 2020). Of those measurements that have been made under ice, many studies report low flux rates (Orihel et al., 2017), while others have measured substantial winter loading (North et al., 2015; Reedyk et al., 2001). Our results provide further evidence that mobilization and release of sediment P are still possible under ice cover. Despite the high flux rates measured under ice, hypolimnetic TP concentrations did not increase from winter to the next sampling event in spring. The winter P fluxes may not have been sustained long enough to cause a noticeable increase in water-column P. Alternatively, the P released under ice cover could have been exported downstream before the spring sampling event or diluted during ice melt (Cavaliere & Baulch, 2020). The relative importance of winter internal loading is likely to be system-specific but to assume that winter P fluxes are negligible risks biasing estimates of annual internal loading.

Sediment core incubations are a common tool for measuring sediment P flux rates (Orihel et al., 2017); however, the approach also has limitations (Ogdahl et al., 2014). The main assumption when using core incubations to quantify sediment flux dynamics is that the conditions in the core are representative of the conditions in the waterbody. In an effort to meet this assumption, we incubated cores at ambient temperature and oxygen conditions at the time of collection, monitoring the temperature, dissolved oxygen, and pH daily in the cores. Overall, the experimental setup mimicked ambient conditions (Appendix S1: Table S1,

Figure S1). We also used measurements from replicate cores and multiple days of incubation to estimate daily mean flux rates at a site for a given sampling event in order to capture small-scale spatiotemporal variability in the estimate while comparing across larger spatial and temporal scales. Additionally, we limited our incubations to 3.5 days in order to minimize artifacts that can occur in long-term incubations such as the depletion of organic matter or other key nutrients. Finally, we compared our core incubation-based flux measurements to TP dynamics in the reservoir as another way to verify that the qualitative patterns we observed in flux rates matched the changes in TP concentration measured in the reservoir. These strategies combined provide confidence that the broadscale spatiotemporal patterns in sediment P flux that we measured reflect the dynamics occurring across sites and seasons in the ecosystem.

Sediment P composition controls flux response to dissolved oxygen

Over the course of the year, we measured internal P loading under a wide range of dissolved oxygen concentrations at the sediment-water interface. Although the dominance of aerobic versus anaerobic internal loading shifted over sites and seasons, both processes were important pathways for P recycling between sediments and the overlying water. In order to understand why sediment P fluxes responded differently to dissolved oxygen conditions across space and time, we measured the chemical composition of the sediment P pool. We hypothesized that this slow variable shapes how fluxes respond to external drivers that alter dissolved oxygen availability. Spatiotemporal variation in sediment P composition corresponded to variation in sediment P flux rates. Specifically, instances of P release under oxic conditions mainly coincided with declines in labile organic P. Sediment P release during hypolimnetic anoxia and the deep site corresponded to decreasing redox-sensitive P concentrations in sediments.

A change in the concentration of a sediment P fraction over time could indicate flux across the sediment–water interface or a transformation within sediments. Evaluating temporal change in both total sediment P and various P fractions helps to distinguish between these processes. At the deep site of the reservoir, change in total and redox-sensitive P concentrations mirrored P flux rates over time. Redox-sensitive P declined steadily from winter to mid-summer and then sharply decreased (35% decrease) from mid- to late summer. The mid-summer sampling event was a hot spot–hot moment of P release from profundal sediments that coincided with hypolimnetic

ECOSPHERE 13 of 16

anoxia at the deep site. The decline in redox-sensitive P from spring to late summer suggests that the high flux rates in mid-summer were the result of the reductive dissolution of redox-sensitive P minerals under anoxic conditions. However, TP only declined from spring to mid-summer, suggesting that some of the redox-sensitive P mobilized between mid- to late summer remained in sediments. The concentration of aluminum-bound P at the deep site followed the inverse pattern of redox-sensitive P. This temporal pattern suggests that a portion of the P mobilized from redox-sensitive minerals may have sorbed to available aluminum oxides rather than being released into the overlying water.

Concentrations of labile organic P in sediments generally increased over the course of the year at all sampling sites, likely due to organic matter sedimentation. However, declines were measured at the shallow and intermediate sites from mid- to late summer, indicating that the elevated rates of aerobic P release measured at these sites in late summer involved P mineralization following the decomposition of labile organic materials. Sediment TP generally decreased during this time as well, specifically from spring to late summer at the intermediate site and from spring to autumn at the shallow site. The decline in TP at these sites extends beyond the short period of decreasing labile organic P concentrations and is likely driven by declines in redox-sensitive P at these sites over the same time. Temporal coherence between sediment P release and declines in sediment total, labile organic, and redox-sensitive P underscores the complexity of P mobilization under oxic conditions and the variety of P species that may be released.

Our hypothesis that there are hot spots and hot moments of internal loading resulting from interactions between sediment P composition and biogeochemical conditions at the sediment-water interface was supported in our study reservoir. We found that anoxic conditions can trigger the rapid mobilization and release of P from redox-sensitive P pools regardless of water temperature. We also measured P release originating from labile organic materials, as well as redox-sensitive minerals under aerobic conditions, and found that these fluxes were enhanced following a storm disturbance. Our findings underscore the importance of considering both aerobic and anaerobic pathways of internal loading, especially in productive waterbodies. Our work supports the idea of a "perpetual cycle of internal P loading" in hypereutrophic waterbodies, as proposed by Song and Burgin (2017). The perpetual cycle describes a positive feedback loop that develops as lakes become increasingly eutrophic. Increased algal production enhances inputs of detritus to sediments, producing a large pool of sediment labile organic P that is susceptible to aerobic release (Baines & Pace, 1994; Frost et al., 2019). Sediment P release may then occur under both anoxic and oxic conditions. High internal P loads sustain frequent algal blooms, the detritus of which further fuels aerobic sediment P release via decomposition and mineralization. This positive feedback loop likely introduces hysteresis to maintain waterbodies in a hypereutrophic state. Clear evidence of sediment P release under both oxic and anoxic conditions in GVL indicates that the reservoir has entered this proposed cycle in which both aerobic and anaerobic internal loading will continue to fuel intense algal blooms.

Scaling fluxes to the whole ecosystem

A hot spot-hot moment is defined as having a disproportionate influence on elemental cycles at the ecosystem scale (McClain et al., 2003). As such, we scaled measured P flux rates to representative areas of the lakebed to estimate P loads and determine how the fluxes we classified as hot spots-hot moments actually influenced reservoir-wide internal loading. Hot spots and hot moments of P release from the shallow and intermediate-depth sites in late summer under oxic conditions produced the greatest total sediment P load to the reservoir over the study period. This substantial P load resulted from both the high flux rates and the broad spatial extent of sediments releasing P at this time. The importance of littoral areas in governing total internal P loads has also been observed in other waterbodies (Tammeorg et al., 2017). High rates of P release from the deep site in winter and mid-summer did not result in large TP loads due to the small area of the lakebed represented by the deep site and sediment P retention at other sampling sites. The scaling results further illustrate how even low rates of P release can result in elevated TP loads if sustained over the entire lakebed. Specifically, we found that low rates of P release across all sampling sites in spring resulted in a high TP load.

Focusing on rates alone may not be sufficient to understand how extreme values of biogeochemical fluxes actually affect ecosystem structure and function. It is essential to scale measurements to the whole system. At the same time, scaling measurements from a single sampling station to an area of the lakebed is fraught with uncertainty. However, we took a conservative approach in assigning representative areas of the lakebed. We also took care to accurately describing the reservoir basin geometry and calculating sediment surface area. As such, we have produced conservative estimates of sediment P loads that can be used to evaluate the ecosystem effects of spatiotemporal variation in P fluxes. Other studies have scaled discrete measurements of sediment P fluxes to larger areas of the lakebed, generally based on

waterbody surface area (Noffke et al., 2016; Scicluna et al., 2015). Our approach to characterizing basin geometry allows for more accurate estimates of sediment surface area and thus scaling at finer spatial resolutions based on water depth.

CONCLUSIONS

Hot spots and hot moments of sediment P release in the study reservoir arose from interactions between the composition of the sediment P pool and external drivers that determined dissolved oxygen conditions at the sediment-water interface. Our findings demonstrate that the magnitude and mechanisms of internal P loading cannot be understood without capturing both seasonal and spatial variations in fluxes and the composition of the sediment P pool as a slow variable. Our understanding of internal P loading in the reservoir would have been very different had we only sampled at one site or in one season. Additionally, scaling flux rates across the lakebed to estimate internal load revealed that even low rates of P release can result in elevated TP loads if sustained over the entire lakebed. Conversely, very high P flux rates do not necessarily produce high TP loads if these fluxes occur over a small area or are balanced by P retention in other regions of the lakebed. These findings illustrate how focusing solely on flux rates without scaling to the whole ecosystem could lead to the misidentification of the main sources and mechanisms of internal loading and ultimately hamper eutrophication management.

ACKNOWLEDGMENTS

This research was supported by the Iowa Water Center's Graduate Student Supplemental Research Competition. Ellen A. Albright was supported by the National Science Foundation Graduate Research Fellowship Program under Grant Number DGE-1747503 and 1744592. Any opinions, findings, and conclusions or recommendations expressed in this material are those of the authors and do not necessarily reflect the views of the National Science Foundation. Support was also provided by the Graduate School and the Office of the Vice-Chancellor for Research and Graduate Education at the University of Wisconsin-Madison with funding from the Wisconsin Alumni Research Foundation. Grace M. Wilkinson was supported by the National Science Foundation Division of Environmental Biology grant numbers. 1942256 and 2200391. Open access funding provided by the Iowa State University Library.

CONFLICT OF INTEREST

The authors declare no conflict of interest.

DATA AVAILABILITY STATEMENT

The data (Albright & Wilkinson, 2021) and analysis code (Albright, 2022) are available from Zenodo: https://doi.org/10.5281/zenodo.6604143.

ORCID

Ellen A. Albright https://orcid.org/0000-0002-6226-9158

Grace M. Wilkinson https://orcid.org/0000-0003-4051-2249

REFERENCES

- Albright, E.A. 2022. "Spatiotemporal Variation in Internal Phosphorus Loading, Sediment Characteristics, Water Column Chemistry, and Thermal Mixing in a Hypereutrophic Reservoir in Southwest Iowa, USA (2019–2020)." AlbrightE/GVL_Internal_P_Cycling-Release-2022 Version 1. Zenodo. https://doi.org/10.5281/zenodo.6604143.
- Albright, E. A., and G. M. Wilkinson. 2021. "Spatiotemporal Variation in Internal Phosphorus Loading, Sediment Characteristics, Water Column Chemistry, and Thermal Mixing in a Hypereutrophic Reservoir in Southwest Iowa, USA (2019–2020) Version 1." *Environmental Data Initiative*. https://doi.org/10.6073/pasta/d3a70c1f0d534cca8bdebd7f7483ef38.
- Baines, S. B., and M. L. Pace. 1994. "Relationships between Suspended Particulate Matter and Sinking Flux along a Trophic Gradient and Implications for the Fate of Planktonic Primary Production." *Canadian Journal of Fisheries and Aquatic Science* 51: 25–36.
- Bernhardt, E. S., J. R. Blaszczak, C. D. Ficken, M. L. Fork, K. E. Kaiser, and E. C. Seybold. 2017. "Control Points in Ecosystems: Moving Beyond the Hot Spot Hot Moment Concept." *Ecosystems* 20: 665–82.
- Bivand, R., J. Nowosad, and R. Lovelace. 2021. "spData: Datasets for Spatial Analysis. R Package Version 0.3.10." https://cran.r-project.org/web/packages/spData/index.html.
- Buelo, C. D., S. R. Carpenter, and M. L. Pace. 2018. "A Modeling Analysis of Spatial Statistical Indicators of Thresholds for Algal Blooms." *Limnology and Oceanography Letters* 3: 384–92.
- Caraco, N. F., J. J. Cole, and G. E. Likens. 1993. "Sulfate Control of Phosphorus Availability in Lakes: A Test and Re-Evaluation of Hasler and Einsele's Model." *Hydrobiologia* 253: 275–80.
- Cardoso-Silva, S., P. A. D. Ferreira, R. C. L. Figueira, D. C. Silva, V. Moschini-Carlos, and M. L. M. Pompêo. 2018. "Factors that Control the Spatial and Temporal Distributions of Phosphorus, Nitrogen, and Carbon in the Sediments of a Tropical Reservoir." Environmental Science and Pollution Research 25: 31776–89.
- Carpenter, S. R. 2003. *Regime Shifts in Lake Ecosystems: Pattern and Variation*. Oldendorf/Luhe: Ecology Institute.
- Carpenter, S. R., and M. G. Turner. 2000. "Hares and Tortoises: Interactions of Fast and Slow Variables in Ecosystems." *Ecosystems* 3: 495–7.
- Cavaliere, E., and H. M. Baulch. 2020. "Winter in Two Phases: Long-Term Study of a Shallow Reservoir in Winter." Limnology and Oceanography 66: 1335–52.
- Corfidi, S. F., M. C. Coniglio, A. E. Cohen, and C. M. Mead. 2016. "A Proposed Revision to the Definition of 'Derecho'." *Bulletin of the American Meteorological Society* 97: 935–49.

ECOSPHERE 15 of 16

- Crépin, A. 2007. "Using Fast and Slow Processes to Manage Resources with Thresholds." *Environmental & Resource Economics* 36: 191–213.
- Filzmoser, P., K. Hron, and M. Templ. 2018. *Applied Compositional Data Analysis with Worked Examples in R. Spring Series in Statistics*. Cham: Spring International Publishing.
- Forsberg, C. 1989. "Importance of Sediments in Understanding Nutrient Cyclings in Lakes." *Hydrobiologia* 176/177: 263–77.
- Frost, P. C., C. Prater, A. B. Scott, K. Song, and M. A. Xenopoulos. 2019. "Mobility and Bioavailability of Sediment Phosphorus in Urban Stormwater Ponds." *Water Resources Research* 55: 3680–8.
- Gakuruh, H. 2017. "Essentials of Data Analysis and Graphics Using R." https://helleng.github.io/Data_Mgt_Analysis_and_Graphics_ R/Data_Analysis.
- Goff, T. C., M. D. Nelson, G. C. Liknes, T. E. Feeley, S. A. Pugh, and R. S. Morin. 2021. "Rapid Assessment of Tree Damage Resulting from a 2020 Windstorm in Iowa, USA." Forests 12: 555.
- Hayes, N. M., B. R. Deemer, J. R. Corman, N. R. Razavi, and K. E. Strock. 2017. "Key Differences between Lakes and Reservoirs Modify Climate Signals: A Case for a New Conceptual Model." Limnology and Oceanography Letters 2: 47–62.
- Horppila, J., H. Holmroos, J. Niemistö, I. Massa, N. Nygrén, P. Schönach, P. Tapio, and O. Tammeorg. 2017. "Variations of Internal Phosphorus Loading and Water Quality in a Hypertrophic Lake during 40 Years of Different Management Efforts." Ecological Engineering 103: 264–74.
- Hudson, J. J., and D. M. Vandergucht. 2015. "Spatial and Temporal Patterns in Physical Properties and Dissolved Oxygen in Lake Diefenbaker, a Large Reservoir on the Canadian Prairies." Journal of Great Lakes Research 41: 22–33.
- Hupfer, M., and J. Lewandowski. 2008. "Oxygen Controls the Phosphorus Release from Lake Sediments—A Long-Lasting Paradigm in Limnology." *International Review of Hydrobiology* 93: 415–32.
- Jensen, H. S., and F. Ø. Andersen. 1992. "Importance of Temperature, Nitrate, and pH for Phosphate Release from Aerobic Sediments of Four Shallow, Eutrophic Lakes." Limnology and Oceanography 37: 577–98.
- Joshi, S. R., R. K. Kukkadapu, D. J. Burdige, M. E. Bowden, D. L. Sparks, and D. P. Jaisi. 2015. "Organic Matter Remineralization Predominates Phosphorous Cycling in the Mid-Bay Sediments in the Chesapeake Bay." *Environmental Science and Technology* 49: 5887–96.
- Kimmel, B. L., and A. W. Groeger. 1984. "Factors Controlling Primary Production in Lakes and Reservoirs: A Perspective." *Lake and Reservoir Management* 1: 277–81.
- Kleeberg, A., A. Freidank, and K. Jöhnk. 2013. "Effects of Ice Cover on Sediment Resuspension and Phosphorus Entrainment in Shallow Lakes: Combining In Situ Experiments and Wind-Wave Modeling." *Limnology and Oceanography* 58: 1819–33.
- Kowalczewska-Madura, K., R. Gołdyn, J. Bogucka, and K. Strzelczyk. 2019. "Impact of Environmental Variables on Spatial and Seasonal Internal Phosphorus Loading in a Mesoeutrophic Lake." International Journal of Sediment Research 34: 14–26.
- Lukkari, K., H. Hartikainen, and M. Leivuori. 2007. "Fractionation of Sediment Phosphorus Revisited. I: Fractionation Steps and

- their Biogeochemical Basis." Limnology and Oceanography: Methods 5: 433–44.
- McCarty, J. A. 2019. "Sediment Phosphorus Release in a Shallow Eutrophic Reservoir Cove." *Transactions of the ASABE* 62: 1269–81.
- McClain, M. E., E. W. Boyer, C. L. Dent, S. E. Gergel, N. B. Grimm, P. M. Groffman, S. C. Hart, et al. 2003. "Biogeochemical Hot Spots and Hot Moments at the Interface of Terrestrial and Aquatic Ecosystems." *Ecosystems* 6: 301–12.
- Mortimer, C. 1941. "The Exchange of Dissolved Substances between Mud and Water in Lakes." *Journal of Ecology* 29: 280–39.
- Murphy, J., and J. P. Riley. 1962. "A Modified Single Solution Method for the Determination of Phosphate in Natural Waters." *Analytica Chimica Acta* 27: 31–6.
- Noffke, A., S. Sommer, A. W. Dale, P. O. J. Hall, and O. Pfannkuche. 2016. "Benthic Nutrient Fluxes in the Eastern Gotland Basin (Baltic Sea) with Particular Focus on Microbial Mat Ecosystems." *Journal of Marine Systems* 158: 1–12.
- North, R. L., J. Johansson, D. M. Vandergucht, L. E. Doig, K. Liber, K. Lindenschmidt, H. Baulch, and J. J. Hudson. 2015. "Evidence for Internal Phosphorus Loading in a Large Prairie Reservoir (Lake Diefenbaker, Saskatchewan)." *Journal of Great Lakes Research* 41: 91–9.
- Nowlin, W. H., J. L. Evarts, and M. J. Vanni. 2005. "Release Rates and Potential Fates of Nitrogen and Phosphorus from Sediments in a Eutrophic Reservoir." *Freshwater Biology* 50: 301–22.
- Ogdahl, M. E., A. D. Steinman, and M. E. Weinert. 2014. "Laboratory-Determined Phosphorus Flux from Lake Sediments as a Measure of Internal Phosphorus Loading." *Journal of Visualized Experiments* 85: e51617.
- Oksanen, J., Gavin L. Simpson, F. Guillaume Blanchet, Roeland Kindt, Pierre Legendre, Peter R. Minchin, R.B. O'Hara, et al. 2019. "vegan: Community Ecology Package." R Package Version 2.5-6.
- Orihel, D. M., H. M. Baulch, N. J. Casson, R. L. North, C. T. Parsons, D. C. M. Seckar, and J. J. Venkiteswaran. 2017. "Internal Phosphorus Loading in Canadian Fresh Waters: A Critical Review and Data Analysis." *Canadian Journal of Fisheries and Aquatic Science* 74: 2005–29.
- Ortiz, D. A., and G. M. Wilkinson. 2021. "Capturing the Spatial Variability of Algal Bloom Development in a Shallow Temperate Lake." *Freshwater Biology* 66: 2064–75.
- Pebesma, E. 2018. "Simple Features for R: Standardized Support for Spatial Vector Data." *The R Journal* 10: 439–46.
- R Core Team. 2019. R: A Language and Environment for Statistical Computing. Vienna: R Foundation for Statistical Computing. https://www.R-project.org/.
- Reedyk, S., E. E. Prepas, and P. A. Chambers. 2001. "Effects of Single Ca(OH)₂ Doses on Phosphorus Concentration and Macrophyte Biomass of Two Boreal Eutrophic Lakes over 2 Years." *Freshwater Biology* 46: 1075–87.
- Scicluna, T. R., R. J. Woodland, Y. Zhu, M. R. Grace, and P. L. M. Cook. 2015. "Deep Dynamic Pools of Phosphorus in the Sediment of a Temperate Lagoon with Recurring Blooms of Diazotrophic Cyanobacteria." *Limnology and Oceanography* 60: 2185–96.

21508925, 2022, 8, Downloaded from https com/doi/10.1002/ccs2.4201 by UNIVERSITY OF WISCONSIN-MADISON, Wiley Online Library on [18/01/2023]. See the Terms

16 of 16 ALBRIGHT AND WILKINSON

Søndergaard, M., J. P. Jensen, and E. Jeppesen. 2003. "Role of Sediment and Internal Loading of Phosphorus in Shallow Lakes." *Hydrobiologia* 506-509: 135–45.

- Song, K., and A. J. Burgin. 2017. "Perpetual Phosphorus Cycling: Eutrophication Amplifies Biological Control on Internal Phosphorus Loading in Agricultural Reservoirs." *Ecosystems* 20: 1483–93.
- Standard Methods for the Examination of Water and Wastewater. 1998a. "20th Edition. Method 4500-P B.5." American Public Health Association, American Water Works Association, and Water Environment Federation.
- Standard Methods for the Examination of Water and Wastewater. 1998b. "20th Edition. Method 4500-P E." American Public Health Association, American Water Works Association, and Water Environment Federation.
- Tammeorg, O., J. Horppila, P. Tammeorg, M. Haldna, and J. Niemistö. 2016. "Internal Phosphorus Loading across a Cascade of Three Eutrophic Basins: A Synthesis of Short- and Long-Term Studies." Science of the Total Environment 572: 943–54.
- Tammeorg, O., T. Möls, J. Niemistö, H. Holmroos, and J. Horppila. 2017. "The Actual Role of Oxygen Deficit in the Linkage of the Water Quality and Benthic Phosphorus Release: Potential Implications for Lake Restoration." Science of the Total Environment 599: 732–8.
- Tammeorg, O., G. Nürnberg, J. Niemistö, M. Haldna, and J. Horppila. 2020. "Internal Phosphorus Loading Due to Sediment Anoxia in Shallow Areas: Implications for Lake Aeration Treatments." Aquatic Science 82: 54.

- Walker, B. H., S. R. Carpenter, J. Rockstrom, A. Crépin, and G. D. Peterson. 2012. "Drivers, 'Slow' Variables, 'Fast' Variables, Shocks and Resilience." *Ecology and Society* 17: 30.
- Walsh, J. R., J. R. Corman, and S. E. Munoz. 2018. "Coupled Long-Term Limnological Data and Sedimentary Records Reveal New Control on Water Quality in a Eutrophic Lake." Limnology and Oceanography 64: S34–48.
- Ward, N. K., L. Fitchett, J. A. Hart, L. Shu, J. Stachelek, W. Weng, Y. Zhang, et al. 2019. "Integrating Fast and Slow Processes Is Essential for Simulating Human–Freshwater Interactions." Ambio 48: 1169–82.
- Wuertz, D., T. Setz, Y. Chalabi, C. Boudt, P. Chausse, and M. Miklovac. 2020. "fGarch: Rmetrics Autoregressive Conditional Heteroskedastic Modelling. R Package Version 3042.83.2." https://cran.r-project.org/web/packages/fGarch/index.html

SUPPORTING INFORMATION

Additional supporting information can be found online in the Supporting Information section at the end of this article.

How to cite this article: Albright, Ellen A., and Grace M. Wilkinson. 2022. "Sediment Phosphorus Composition Controls Hot Spots and Hot Moments of Internal Loading in a Temperate Reservoir." *Ecosphere* 13(8): e4201. https://doi.org/10.1002/ecs2.4201